Techno–economic Potential of Battery Energy Storage Systems in Frequency Response and Balancing Mechanism Actions

IET Research Journals

Research Article - Review Submission

IET Journals
The Institution of Engineering and Technology

ISSN 1751-8644
doi: 0000000000
www.ietdl.org

Techno–economic Potential of Battery Energy Storage Systems in Frequency Response and Balancing Mechanism Actions

Desen Kirli [1*], *Aristides Kiprakis*[1]

[1] *Institute for Energy Systems, School of Engineering, University of Edinburgh, Faraday Building, King's Buildings, Colin Maclaurin Road, Edinburgh, EH9 3DW, United Kingdom*
** E-mail: desen.kirli@ed.ac.uk*

Abstract: Batteries offer a combination of balancing and regulation services within a smart grid to improve its resilience and flexibility. Maintaining an acceptable state of health and the highest rate of return requires dynamic modelling of the asset and rigorous optimisation. We compare the technical cost and economic benefit of battery employment in dynamic frequency and balancing mechanism actions in a smart grid. We use the services procured by National Grid in the UK as a case study but the methodology is globally applicable, including developing grid infrastructures. Our methodology yields the most optimum scenario of service participation, accounting for the dynamic degradation and considering variable pricing of electricity throughout the day. Additionally, it advises the most optimal despatch schedule and price declarations for the battery over the course a day and a year, employing Particle Swarm Optimisation algorithm and historic data. Our results demonstrate that ordinarily frequency response is preferred due to its lower technical toll and payments for availability rather than despatch. However, the proposed despatch schedule including both services provides the highest profit. We anticipate this methodology to become the basis for more sophisticated battery models that integrate the service despatch optimisation, dynamic lifetime degradation and economic analysis.

1 Introduction

In response to carbon emission and greener electricity production targets, the energy mix in the UK is changing to integrate newer and cleane444444r electricity generation technologies on a conventional electricity grid. As the capacity of generation from wind, solar and interconnection increase, the transmission system operator National Grid (NG) predicts lower system stability and higher fluctuations in frequency and generated power [1]. As a consequence, there is a growing need for faster balancing action in order to stabilise the system frequency and deliver electricity within the regulatory frequency range.

Battery energy storage systems (BESS) offer a solution that responds to this problem and allows further integration of renewable energy technologies by making the electricity grid smarter and more flexible. Fig. 1 presents the role of BESS on both demand and balancing action in a model smart grid, following the approach by [2].

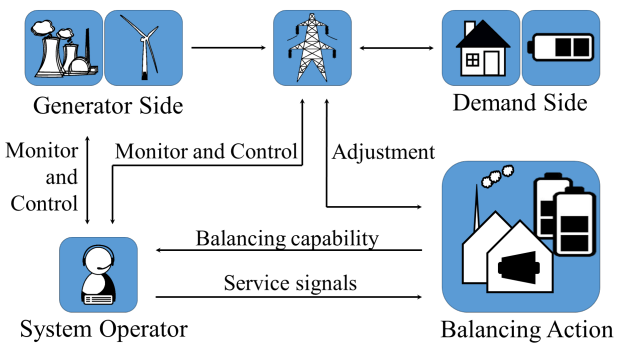

Fig. 1: Representation of a smart grid scenario with BESS installed on both demand and balancing action sides

It is also a relatively low-carbon solution in comparison to the conventional means of operating fossil-fuel generators at part-load [3]. The latest services report by NG states that the only two undersubscribed services are Dynamic Firm Frequency Response (dFFR) and Balancing Mechanism (BM) actions. Hence, this paper focuses on these two ancillary services to help balance the transmission system using BESS. The methodology yields the most optimum scenario of service participation, accounting for the dynamic degradation of the battery and considering variable pricing of electricity throughout the day and the year. The most significant points of contribution to knowledge are as listed:

- The most profitable despatch schedule for a 1MW/1MWh lithium-ion BESS, for the working and non-working day profiles of every month in a year, using Particle Swarm Optimisation to maximise profit and minimise service penalties and idle time whilst respecting all operational and technical constraints.
- A dynamic lifetime degradation model that is based on real usage data provided by four battery companies.
- Bid and offer pricing optimisation with respect to the realistic battery cycling and lifetime constraints for participation in Balancing Mechanism using real imbalance pricing and market data for one year.
- A realistic battery frequency response model (indexed to the rate of change of frequency) that uses real system frequency data, recorded in Great Britain, and takes NG's dFFR regulations and penalties into consideration.
- Calculation of levelised cost of storage using the capital and operational costs provided by four BESS companies and comparison with the ranges published in academic literature and by industry.

- Techno-economic analysis over the lifetime of BESS that includes the break-even analysis, net present value at the end of lifetime and average daily state of charge variations which prove the economic viability of the simulated 1MW/1MWh BESS unit.

2 Previous work

As studied by Doherty *et al.* [4], the "non-synchronous connection" of solar and inverter-connected wind generation deliver little to no inertia response to the grid. Thus, growth in renewable integration decreased the overall system inertia, resulting in higher frequency fluctuations and made management of dynamic system frequency more challenging. The other major cause of system imbalance is the uncertainty associated with the prediction of electricity production from renewable energy sources. A good example is wind generation in the UK. As the actual wind out-turn deviates from the initial and even the latest forecast, the use of BESS for firming the output capacity was repeatedly researched to minimise this problem [5]–[8]. Hence, the demand for BESS is expected to grow as generation from renewable energy technologies increase.

The most recent survey of literature revealed no studies in the field of BESS participation in the British BM market. Hence, we believe that this paper is a pioneer for the comparison of BM and dFFR actions and using a BESS in the UK electricity market as a case study. the choice of frequency response service for this techno-economic analysis, Sami *et al.* [9] and existing commercial-scale applications prove that the grid-scale BESS can offer frequency response faster than conventional "frequency-sensitive generators". The "coordinated adaptive droop control" by Sami *et al.* [9] offers the best approach with the least technical cost imposed. It dictates that a higher rate of change of frequency activates a higher portion of the committed unit approach. This method is modified with the NG dFFR rules and employed in this paper. Currently, the grid-connected 1MW li-ion BESS in Zurich provides the most recent and comprehensive comparisons of the ex-ante and ex-post simulations. It uses a varying roundtrip efficiency of 80-90% depending on power output and examines the effect of frequency response actions on the state of health [10]. Although both [9] and [10] examine the simulation techniques of grid frequency response, neither investigate the economic gain nor compare it with other services such as BM. In contrast, Gundogdu *et al.* [11] report the revenue from a similar frequency response (i.e. enhanced frequency response) procured by NG. However, it still does not compare the revenue from frequency and arbitrage or BM services. Instead, it studies triad avoidance as an alternative service which is available between November and February. As there is no limit when the BESS can take part in BM or dFFR, it results in a more complex scheduling problem that is addressed by an optimisation algorithm in this paper. In summary, in most of the studies, including the ones mentioned, formulation of the technical degradation or remaining cycles in the lifetime is overlooked. Lastly, none employ optimisation algorithms such as particle swarm optimisation (PSO) as they do not consider scheduling of different services at all.

On the other hand, there is some research that solely concentrates on scheduling and integration of operational limits. For example, Duggal *et al.* [12] investigate the effect that the method of scheduling has on the battery depth of discharge (DoD) and lifetime whilst meeting the power demand using thermal generation and BESS. It has a similar approach to the technique employed in this paper as it takes efficiency and state of charge (SoC) limits into account. [13] presents two novel SoC forecasting models and a method to calculate their optimal parameters. This work treats cycles and degradation in detail as well. However, it does not consider the effect of service participation. In the model proposed in this study, there is no need for forecasting as it utilises historic data. Nevertheless, it forms the basis for forecasting models of service participation which could employ the SoC forecasting techniques from [13].

Regardless of the asset size and type, the topic of scheduling is investigated in [14]–[24] which all aim to optimise different things such as reducing bills or avoiding penalties. [14] and [15] investigate the optimal operation strategy for BESS using the ancillary services in the U.S.A. as a case study. The former investigates the scheduling of distributed battery assets from the aggregator's perspective. The latter makes a risk-based analysis using an optimisation algorithm. However, the requirements and penalty system of the services do not align with NG. [14] only examines the benefit of arbitrage and overlooks the potential of frequency services. However, it takes a similar approach in terms of choosing prices to take part in the BM services through optimisation yet it studies the problem as an aggregated response of existing distributed assets instead of viewing it from the perspective of a battery owner or an investor. Kazemi *et al.* [15] use robust optimisation formulation to obtain the optimal bidding strategy for typical reserve and frequency markets in the U.S.A. Nonetheless, [15] considers only day-ahead markets. Similarly, [16] models battery demand uncertainty using the same optimisation technique. It proposes the use of this algorithm in conjunction with the model of electricity pricing uncertainty for battery swapping stations. They neglect to integrate a data-driven dynamic degradation model, limits of operational warranty, lifetime analysis in cycles and operation till end of life. Several other researchers also study scheduling but the asset of interest differ and often is a group of smaller distributed storage systems [17]–[20]. Using the aggregated capacity of electric vehicles, [17] proposes a bidding of ancillary services in regulation and spinning reserve markets. This approach accounts for market uncertainties using the technique of fuzzy optimisation. Similar to [14], it views the problem as an aggregator. [18] also uses optimisation for demand response scheduling and utilises the dynamic programming method. Motalleb *et al.* [18] consider two parameters in their optimisation which are operation under normal conditions and during contingency events as their research focus on electric water heater and batteries. This contrasts with the scheduling of the grid-scale BESS which is used to maximise profit. [19] uses genetic algorithm to perform scheduling optimisation of residential BESS. However, the BESS do not export electricity to the grid and the objective is to decrease household bills. [20] develops a stochastic optimisation framework for battery operation. It aims to execute load peak shaving both as day-ahead and near real-time actions at distribution level.

[14]–[20] each have a single objective and use numerous optimisation techniques that range from genetic to robust optimisation. Nonetheless, the main aim of the research undertaken is to perform a multi-objective optimisation. Hence, the multi-objective optimisation methodology followed by [21]–[24] is analysed which all employ PSO. While Jinlei *et al.* [21] use PSO to minimise the operating cost of second use BESS using various constraints, Rodriguez-Gallegos *et al.* [22] employ it to reduce system cost and control scheduling. [24] employs this meta-heuristic algorithm for battery sizing in stand-alone hybrid systems. In summary, the studies reviewed do not compare the same services as this paper, use a dynamic degradation model, perform multi-objective optimisation scheduling for the lifetime of the BESS or evaluate the services in a techno-economic manner.

In this paper, the economic benefit and technical cost of participating in BM and dFFR services are compared, using real historic data for both system frequency deviation and imbalance pricing. The undertaken research is a pioneer in addressing the gap in literature regarding the techno-economic assessment of smart grid services over the BESS lifetime (i.e. participation in which service or service combination would result in the highest profit whilst respecting the limits of battery degradation and operation) and long-term scheduling. The performance of each service is quantified and analysed using various criteria such as the number of cycles completed in the service, duration of commitment, price per MWh, total revenue in a year and 10 years. Whilst the ideal service would cause negligible degradation and offer the highest profit rate, in this case, an optimised participation in both services results in the best degradation to profit ratio. Another contribution to knowledge is the formulation of the multi-objective function that employs the PSO algorithm in order to optimise the scheduling and obtain the highest profit with the minimum idle time whilst ensuring 10 years of operation under warranty. It is also notable that the optimisation is performed respecting the operational constraints, technical limitations and service regulations which are obtained from various sources that include four BESS

companies, NG and research publications from prestigious journals. One notable constraint is the dynamic battery degradation which is formulated using real degradation data from the BESS companies, adopting the method of curve fitting, and applied to each service using the programmed cycle counter. This results in a realistic degradation over 10 years on the granular scale of one cycle. The results are presented and discussed in Section 4. As this paper compares the individual service participation with the optimised schedule where the BESS takes part in both services, it is anticipated that it would be useful for aggregators, battery owners and investors. In addition, it presents the optimal scheduling for working and non-working days for each month of the year which advises the battery owner for participation in two under-subscribed service using real historic data. It is expected that the proposed methodology would become the basis for more sophisticated battery models that integrate service despatch optimisation, dynamic lifetime degradation and economic analysis employed in this paper.

3 BESS modelling and simulation

3.1 Basic Assumptions

When modelling the behaviour of BESS, several static constraints become dynamic over time even if perfect environmental conditions are assumed. This is due to technical degradation over time. Parameters such as efficiency, charge density and lifespan decrease and self-discharge rate increases. Hence, the operation conditions of BESS (i.e. allowed cycles of operation per year, power output and SoC management technique) are crucial for its overall efficiency and lifetime as discussed in [25], [26]. Previous analysis of industry trends has led to the following technical assumptions. Using the outcomes of [27] and [28], the BESS was chosen to be lithium-ion due to the combination of commercial maturity and higher life cycle. The simulated BESS has a 1MW and 1MWh rating. It has a 60% DoD (i.e. battery is discharged to 20% and recharged to 80%). It has a roundtrip efficiency ($\eta_{roundtrip}$) of 90%. As there was no other data provided by the battery manufacturer regarding specific charging and discharging efficiencies, both were assumed to be the same. In addition, the operational constraints include a limitation of 500 cycles per year in order to operate under a 10-year warranty.

Lastly, for the degradation pattern of the BESS, only 12 data points of normalised capacity were provided by the battery manufacturer. The first 11 points covered 0 to 1000 cycles and the last point represented the capacity at the last allowed cycle of operation, the 5000th cycle. As discussed in [12] and [29] degradation diagnostics of lithium-ion cells depend on numerous factors such as exposure to environmental conditions (e.g. temperature), operation pattern and numerous chemical interactions. For the purpose of this study, the individual effects of these factors are discarded. Various battery degradation models such as [31] use the curve fitting model to calculate the remaining battery lifetime ($L(x)$) depending on battery-specific parameters (i.e. a and b) and DoD denoted by x in (1).

$$L(x) = \frac{a}{x^b} \tag{1}$$

Several experimental studies such as by Gao *et al.* [31] and Ando *et al.* [32] also examine li-ion degradation considering different variables such as SoC windows. Nevertheless, both only demonstrate result for under 3500 cycles. The most applicable studies found were the phenomenological model for cyclic ageing by Narayanrao *et al.* [33] (which was implemented in the battery module of COMSOL) and the experimental results published by NASA [34] as both studies were in agreement and provided for our 5000-cycle operation scenario. The degradation curve published by Narayanrao *et al.* was found to be the closest match for the degradation simulation of the BESS.

The system data and the most significant assumptions are summarised in Table 1. As the main objective is to produce a techno-economic BESS model that takes part in dFFR and BM services, the network constraints are neglected and operational constraints and service regulations were prioritised instead. The BESS is assumed to be connected at transmission level on the balancing action side rather than at distribution level on the demand side as shown in Fig. 1.

3.2 Balancing Mechanism Simulations

To participate in BM, a BESS would act as a generator following the power ramp-up and ramp-down restrictions of NG [35]. Ideally, BESS would recharge at a lower price for a greater economic benefit. This service is tendered for half-hourly periods also known as settlement periods (SPs). To participate in BM, each unit has to declare a discharge price (i.e. the amount that the unit gets paid to discharge) and a charge price (i.e. the amount that the unit pays to recharge) [36]. If the instantaneous market prices to export (i.e. offer price) and import (i.e. bid price) cross the set thresholds (i.e. discharge and charge price), the unit gets activated [36].

3.2.1 Simulation Architecture: As illustrated in Fig. 2, the simulation of the BM service uses a data set of the accepted bid and offer prices to calculate the profit and the number of cycles completed. For this simulation, certain constraints were used such as optimum charge and discharge price which required the deployment of a PSO algorithm prior to running the *BM Simulator*.

Table 1 Summary of system data and assumptions

Parameter	Unit	Value or Type
Rated power	MW	1.00
Capacity	MWh	1.00
Cell type		Li-ion
Roundtrip efficiency	%	90.00
Depth of discharge	%	60.00
Lifetime	Cycles	5000

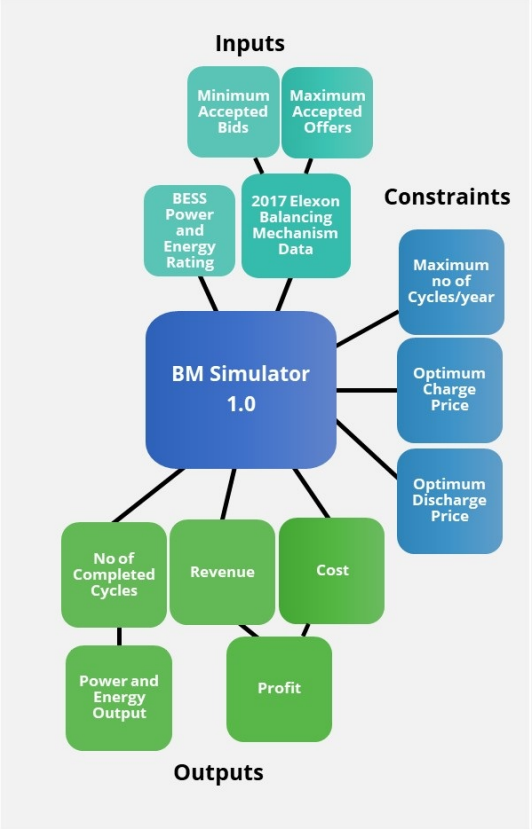

Fig. 2: Inputs, output and constraints of *BM Simulator*

3.2.2 Optimisation of Discharge and Charge Prices: The annual BM profit seems to increase as discharge price decreases (i.e. more offers are accepted and more electricity is sold). As the annual profit is a function of both charge (CP) and discharge price (DP) (i.e. annual profit is the difference of discharge revenue and charge cost over a year), the PSO algorithm was used to maximise the annual profit. The objective function of the PSO algorithm can only be minimised, thus the negative of the profit function (i.e.$-Z(P_c, P_d)$) was used to spot the global minimum, hence the global maximum profit of £78k/year. In order to operate under the 10-year warranty, the operational limit of maximum 500 cycles per year was declared as a constant constraint in the optimisation code. This required programming of a cycle counter, as shown in (2).

$$n = \frac{1}{2} \cdot \sum_{t} m_d + m_c \tag{2}$$

hence,

$$n_{day} = \frac{1}{2} \cdot \sum_{t=1}^{48} m_d + m_c \tag{3}$$

where n denotes the number of cycles in a day. Hence, n_{day} is the cycles in a day in (3). t represents an SP which adds up to 48 in a day. m_d and m_c are discharging and charging actions completed. When power is exported during an SP, m_d and m_c are equal to 1 and 0 respectively. When power is imported, it is vice versa. For instance, for a BESS with maximum SoC, two sets of discharges (i.e. $2.m_d$ would be required to reach the minimum.

When the BESS is triggered to operate, the type of its operation is documented for each SP as 1 (i.e. in action) and 0 (i.e. not in action) in both discharge and charge data sets (e.g. if discharging, SoC: 100%→50%, m_d=1 and m_c=0). Hence, the programmed daily cycle counter divides the total of the actions by 2. The number of cycles for various DP and CP combinations is illustrated in Fig. 3. This exhibits that in order to achieve the global maximum profit, 682 cycles would have to be completed annually. The DP and CP combinations of £116.00 and £0.00, £124.00 and £5.00 and lastly £125.00 and £10.00 provide the highest number of cycles, below 500 per annum.

As shown in Fig. 4, when the 500 cycles/year constraint was introduced to the optimisation algorithm, the global maximum point was relocated to the first local maximum point (£66.2k) - See Local Maximum 1 in Fig.4.

Introducing the operational limitation decreased the number of cycles by 17% at the cost of diminishing the annual profit by 15%. In spite of this, the average value of profit earned per cycle increased from £114.61/cycle to £132.40/cycle, making it more effective in terms of techno-economic performance.

3.3 Dynamic firm frequency response simulations

When participating in dynamic frequency response, a BESS has to charge at high frequencies (i.e. act as a load when f>50Hz) and discharge at low frequencies (i.e. act as a generator when f<50Hz). It has to quickly alternate between actions to counter-act frequency deviations from 50Hz.

3.3.1 Simulation architecture: The *dFFR Simulator* alters the power and energy output of the BESS in relation to the past frequency data to simulate how a BESS would have responded in real life. This involved programming a droop that correlated the power output to the rate of change of frequency. Similar to the *BM Simulator*, this code also outputs profit and number of cycles completed as shown in Fig. 5.

3.3.2 Event-based RoCoF–indexed droop: Simulating this service involved selection of an SoC management approach. Using the "coordinated adaptive droop control" approach of Sami *et al.* [9], a RoCoF–dependent droop was designed which regulates the output from the BESS according to the rate of change of the frequency – See Fig. 6. As proven by Sami *et al.* [9], this strategy is the least taxing for the BESS.

In the dFFR service, the battery is allowed to charge or discharge in order to return to its initial SoC either at the end of the 4-hourly commitment blocks or after responding to a frequency event. However, this has to be performed at very low C-ratings (e.g. 0.2) to ensure that charge or discharge behaviour of the BESS does not augment a frequency deviation. The BESS is only activated when the system frequency exceeds the deadband of 50Hz $\pm$ 0.015 [37], [38].

3.3.3 Long-term dFFR simulation and pricing: Regarding the long-term dFFR simulation, three significant aspects have to be considered. These are the calculation of failure rate, obtaining the number of cycles completed and the pricing. The 2015 system frequency data (at the sampling interval of 15 seconds) is used as the input to the simulator which output the following; (1) the failure rate and (2) the number of completed cycles. Failure in this concept is defined as the being unable to deliver at least 90% of the contracted capacity under a second [38]. A record of more than 10% failure rate may lead to various penalties hence, through long-term simulations performance within the permitted rate is ensured. Participation in dFFR for a year resulted in only 60 cycles per year. Regarding the pricing of the dFFR service, it should be noted that dFFR is contracted through private bi-lateral agreements with NG and the availability price was assumed to be £12/MWh. Unlike BM, the units in dFFR are awarded for being available rather than active. Moreover, there is no recharging cost when participating.

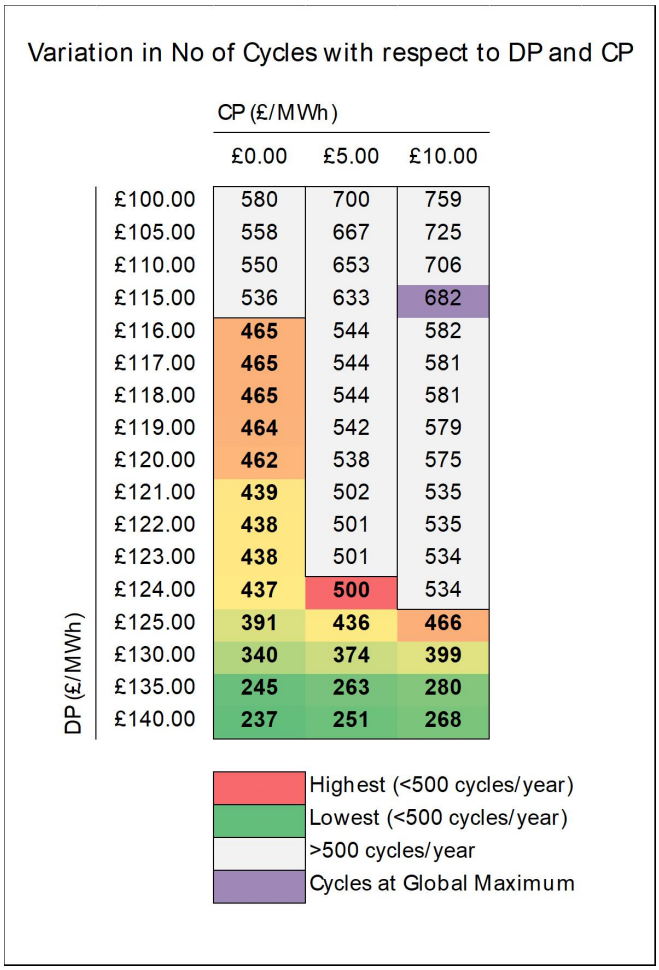

Fig. 3: No of cycles per year for different combinations of discharge and charge prices

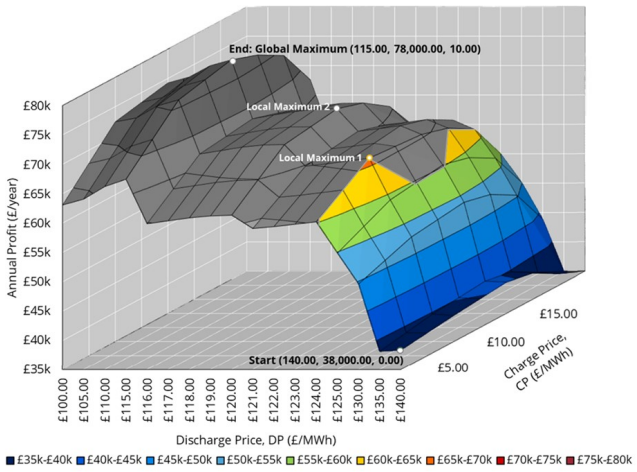

Fig. 4: 3D plot of the annual BM profit function (z-axis) and its variables; discharge (x-axis) and charge price (y-axis). The start point (green circle), local minima (amber circles) and global minimum (red circle) are shown which correspond to maximum profit. The colourful section illustrates the portion below the 500 cycles/year constraint

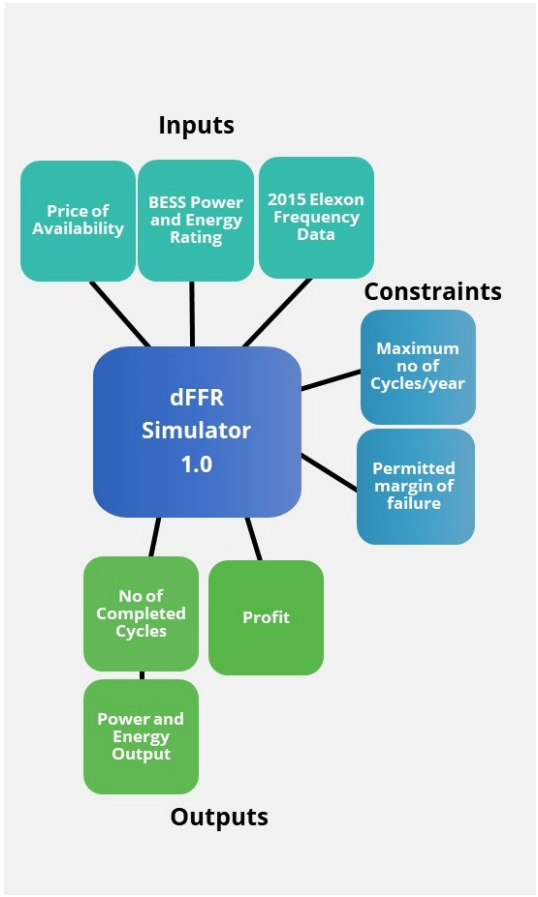

Fig. 5: Inputs, output and constraints of *dFFR Simulator*

3.4 *Despatch scheduler*

This section details the strategy employed to maximise the profit and minimise idleness through timely participation in both BM and dFFR services. It describes the programming technique of the decision algorithm, implementation of PSO and the results from the optimisation algorithm.

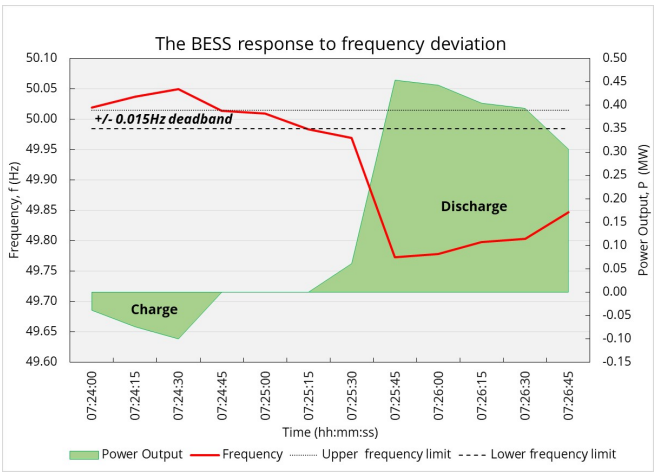

Fig. 6: The programmed droop that controls the BESS response to frequency deviations

BM and dFFR services are tendered separately. dFFR is tendered in blocks of 4 hours (i.e. 8 SPs) and BM is offered in half–hourly SPs. The algorithm analyses the potential profit from dFFR and BM and then compares them to decide on which service to take part in. As there are 6 dFFR blocks in a day, there are 64 (i.e. 2^6) possible combinations in each day which adds up to 23,360 possibilities in a year (i.e. when analysed on a daily basis).

The analysis on dFFR profit showed that the low dFFR service was required more frequently and entering a dFFR block with an SoC of less than 50% increased the simulated failure rate up to 20% (i.e. the BESS could not discharge to counter-act a low-frequency event because of the insufficient SoC level). This significantly reduces the dFFR profit as NG tolerates a maximum of 10% failure rate and decreases the probability of the asset to be chosen by NG in the future dFFR services [38]. Consequently, the SoC limit was declared as the primary decision factor.

3.4.1 Final architecture: Fig. 7 illustrates the decision-making steps of the algorithm. This is performed at the end of each block to determine the service in the one ahead. This decision employs both (1) operational and (2) economic comparisons as shown in Fig. 7. The former requires 50% or more SoC to allow profit comparison between dFFR and BM. If this condition is not satisfied, then the next service is BM. If the SoC is over the threshold, the potential profit from each service is compared. Hence, the next service is the one with the highest profit.

The decision algorithm described above is employed 6 times a day which introduces 64 possible scenarios per day. Therefore, the PSO algorithm was utilised with an objective function to maximise the total profit and minimise the duration of inactivity.

The SoC counter also had to be integrated into the optimiser to ensure that the number of cycles/year and SoC limits were globally declared variables with inequality constraints (e.g. SoC being equal to or more than 50% is an inequality constraint). The major advantage of using PSO for the application was that it is still faster than trying out 64 different combinations manually. Another advantage is that it eliminates the aspect of human error. The reason why PSO was preferred over other techniques was due to its superiority solving in multi-objective optimisation problems with constraints from varying natures, such as equality and equality, as discussed by [21]–[24]. This is detailed in Section 2 and 3.4.2.

3.4.2 Implementation of PSO and an example of unoptimised vs. optimised response: In the unoptimised scenario (See Fig. 8.a), the decision algorithm compared the service profits (i.e. SoC condition was already satisfied) and the BESS was advised to participate in dFFR in Block 1. As the SoC condition was still obeyed and the potential BM benefit in Block 2 was higher than the dFFR one, the decision algorithm directed the BESS to take part in BM. Nevertheless, this resulted in an SoC below 50% and redirected

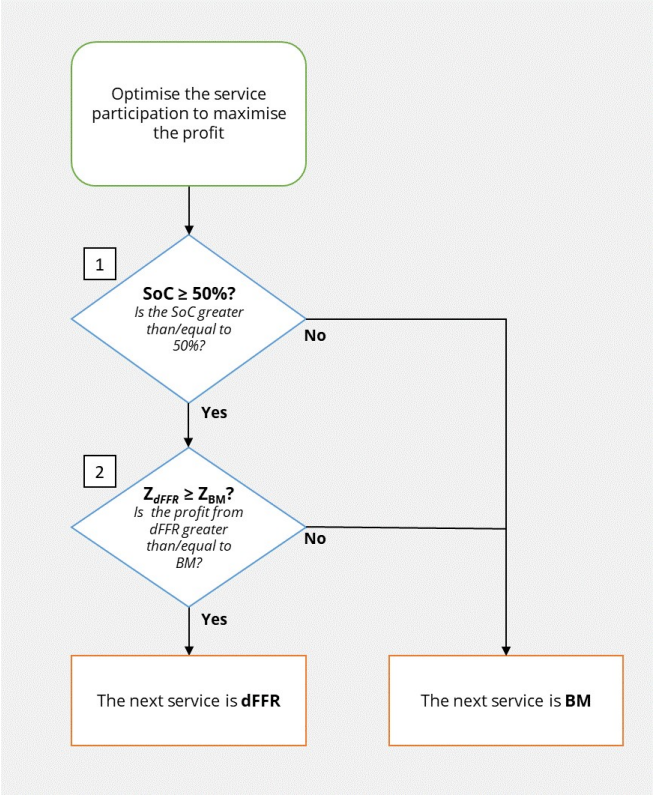

Fig. 7: A flowchart that represents the two-stage decision algorithm which chooses the optimal service to commit to in the next block, depending on a technical and economic parameter. This decision depends on (1) the state of charge and (2) profit comparison of BM and dFFR for the next block

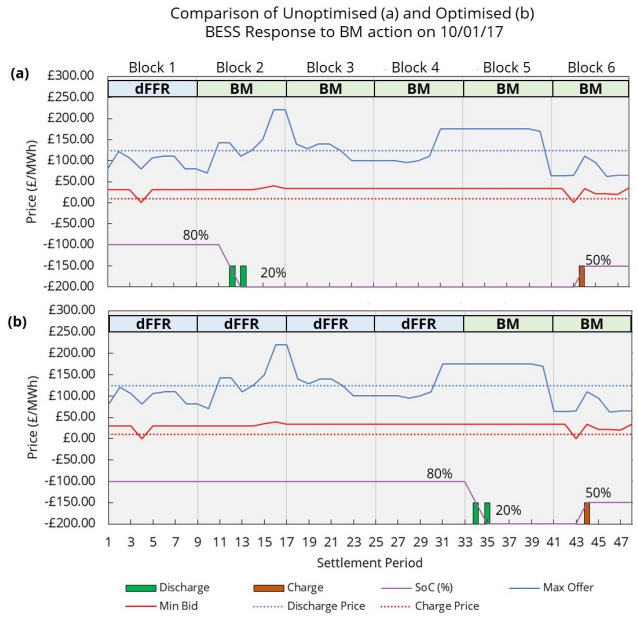

Fig. 8: A comparison of (a) unoptimised and (b) optimised BESS response to pricing profile on 10/01/17. It shows the elimination of idle time, decrease in time spent with SoC<50% and hence the increase in profit when PSO was employed

(a) The unoptimised response that takes part in dFFR in Block 1 and BM in the next 5 blocks with 3 blocks of idle time.

(b) The optimised response that participates in dFFR from Block 1 to 4 and in BM for Block 5 and 6 with no idle time

the BESS back into BM for Block 3. As the bid price did not fall below the declared CP till Block 6, the BESS was idle during the 3 out of 6 blocks.

When this algorithm employs PSO, the optimised scenario as shown in Fig. 8.b was achieved. The exact amount of profit earned in Block 2 of the unoptimised scenario could actually be relocated to Block 5. This way, the first 4 blocks can participate in dFFR and make more profit rather than just being idle.

As there are multiple objectives involved (i.e. minimising idle time and maximising profit), PSO was employed following the previous work from [21]–[24] and the example from the field of flexible manufacturing systems in [39]. Jerald *et al.* [39] use PSO to minimise idle time and penalties incurred. Their work proves that in comparison to the genetic, simulated annealing and memetic algorithms, PSO performs better at multi-objective optimisation where the objectives involve minimising penalties and total machine idleness in their research [39]. Their objectives are very similar to the ones in this study which are namely maximisation of profit and minimisation of idle time by reducing the time spent at an SoC less than 50%.

In this analysis, various constraints are considered that range from the state of charge limits to the number of cycles completed per year. In addition, there are two factors that are required to be optimised simultaneously which are namely maximisation of profit and minimisation of idle time through decreasing the number of actions that result in a low state of charge at the end of the block. These aspects make the problem multi-objective with numerous constraints. In order to implement this, the multi-objective PSO with constraint support was used with no other modifications. This was deployed on *Python* using the *PySwarm* package. Prior to the statement of the objective function, the underlying formulations must be analysed. As previously mentioned, maximising profit is one of the goals as the aim of this research to assess the techno-economic viability of using a BESS for smart grid services. Thus, profit from each service is computed using (4) for BM and (5) for dFFR.

$$Z_{BM} = \frac{1}{2}\left(P_d \cdot \sum m_d - P_c \cdot \sum m_c\right) \tag{4}$$

$$Z_{dFFR} = \frac{P_{dFFR}}{2} \cdot \sum m_{dFFR} \tag{5}$$

where Z_{BM} and Z_{dFFR} represent BM and dFFR profit respectively. P and m denote price and action taken in half a cycle. The subscripts d, c and $dFFR$ correspond to discharge, charge and dFFR respectively. Both formulas employ price and time variables in units of £/MWh and SPs.

$$Z_{tot} = Z_{BM} + Z_{dFFR} \tag{6}$$

Hence, the total profit, Z_{tot} is the summation of the individual contribution of each service as shown in (6).

$$s < 50\%, \quad T_{idle} = t_d - t_c \tag{7}$$

In (7), s represents SoC and T_{idle} is the number of the blocks spent idle which occurs when SoC is less than 50% and the conditions for the DP and CP of the BESS are not satisfied. It should be noted that a block is defined as 8 SPs. t_d and t_c represent the block number where the last action is discharging or charging. For these variables to be registered, there should be at least one block spent with no activity (i.e. m_c=0, m_{dFFR}=0 and m_d=0 for a block) after the discharge that results in a low SoC. This leads to the battery sitting idle for various blocks. Hence, to prevent this, idle time was minimised by incorporating (7) into the combined objective function (COF).

$$min \quad COF = \mathrm{w}_1 \frac{T_{idle}}{T_{tot}} + \mathrm{w}_2 \frac{Z_{\max} - Z_{tot}}{Z_{\max}} \tag{8}$$

where w_1 and w_2 are the weighting factors assigned to each objective. The first term enables the minimisation of idle time divided by the total number of blocks in a day (i.e. T_{tot}=6). Similarly, the second term represents the maximisation of profit.

The optimisation problem is presented in (8) where the overall aim is to minimise the COF. The COF is formulated using the scheduling example from [39] where each component is given a weighting factor. Following the suggestion by Jerald *et al.*, both were set to 0.5. Varying weighting factors would require a detailed sensitivity analysis which is beyond the scope of this work.

One of the most significant constraints for operation is the SoC limits that are expressed in (9). Cycle restrictions for a year and the entire lifetime are expressed below in (10) and (11).

$$\mathrm{s}_{\min} \leq s \leq \mathrm{s}_{\max} \tag{9}$$

As previously stated, the SoC (i.e. s in (9)) limits are declared as $\mathrm{s}_{\min}$=20% and $\mathrm{s}_{\max}$=80% in the simulations.

$$\sum_{N=1}^{365} n_{day} \leq 500 \tag{10}$$

$$\sum_{N=1}^{3650} n_{day} \leq 5000 \tag{11}$$

where N is the number of days. The calculation of n_{day} is shown previously in (3). The constraint shown in (10) ensures operation under warranty as it limits the number of cycles to 500 per year. (11) states the lifetime limit of 5000 cycles.

4 Results

This section presents the results obtained by employing each of the three algorithms, namely *BM Simulator* 1.0, *dFFR Simulator* 1.0 and *Despatch Scheduler*. It provides an overall techno-economic evaluation of the proposed BESS over its lifetime which includes a 10-year forecast of profit, a break-even analysis, determination of payback period and evaluation of technical performance. Additionally, the levelised cost of storage is computed in pursuance of further proving the reliability of the simulation results.

4.1 Techno-economic comparison of BM and dFFR

The *BM Simulator* and *dFFR Simulator*, which are detailed in Section 4.2 and 4.3 respectively, were individually run using data collected over a year in order to represent exclusive participation in each service. This yields the comparison of only BM action for one year and sole dFFR participation in the same year. In Table 2, the techno-economic comparison of the two scenarios is presented where the BESS only takes part in BM in the first scenario and solely in dFFR in the second one. It is explicitly demonstrated that annual profit from dFFR is 1.4 times higher than the one from BM. Also from a technical perspective, dFFR requires only 60 cycles per year which possibly lengthens the lifetime of the battery to over 10 years. Even without the 500 cycles/year constraint for BM, dFFR is still more profitable. On average, participation in dFFR produces almost £5 more per MWh than BM. Hence, it is concluded that the overall participation solely in dFFR is techno-economically more beneficial than in BM.

Table 2 A techno-economic comparison of dFFR and BM services

Parameters	Unit	BM	dFFR
Discharge/Availability Price	£/MWh	124.00	12.00
Charge Price	£/MWh	5.00	0.00
Annual Revenue	£/year	69,200.00	94,600.00
Annual Cost	£/year	3,000.00	0.00
Annual Profit	£/year	66,200.00	94,600.00
Avg. Hourly Profit Rate	£/MWh	7.56	12.00
Avg. Profit Rate during Committed Hours	£/MWh	57.16	12.00
No of cycles/year	Cycles	500	60
Active hours in a year	%	13	95

Nevertheless, it should be noted that the BESS reacts to any frequency change outside the 30 mHz deadband when committed to the dFFR service. This means that it is actively charging and discharging during the majority of the time, whereas the battery is only operating during 13% of the time in BM action. This results in BM providing a net profit of £57.16 for each hour spent discharging which is 5 times the value earned per hour of dFFR participation. The average profit rate during committed hours for BM (i.e. £57.16/MWh) is calculated by dividing the total profit earned from BM action by the number of hours spent discharging whereas the average profit rate (i.e. £7.56/MWh) is calculated by dividing the total profit by the number of hours in a year. The former provides a higher value since the bids and offers of the BESS are accepted only 13% of the time. Both values are the same (i.e. £12.00/MWh) for dFFR as the payment is for availability rather than despatch. This suggests that there is a higher profit potential in BM during certain times of the day. Hence, the profit earned is maximised through adjusted participation in both of these services as previously discussed.

4.2 Results from the Despatch Scheduler

Once the yearly service benefits were computed, the results were used for comparison against exclusive participation in BM and dFFR. The optimised participation provides 20 and 50% more profit than dFFR and BM respectively. The total profit of £113,000 consists of both dFFR and BM participation which accounts for 16 and 84% of the sum respectively. In its lifetime, the battery spends 88% of its 5000 cycles when participating in BM. On the other hand, only 30% of the total time is spent in BM.

The despatch schedule (See Fig. 9) exhibits a strong dFFR presence in the first 3 blocks (i.e. 12 hours, 00:00-12:00). Apart from an exception in May, all other profiles strongly suggest participation in dFFR again in Block 4. On the other hand, Block 6 always employs BM. This is because the bid prices are usually the lowest in Block 6, making it an ideal block for charging up before the next day. The variations in Block 5 are mostly dependent on BM pricing rather than the SoC$\geq$50% limit for participation in dFFR.

Lastly, Fig. 10 shows the variation in SoC when the BESS participates in both BM and dFFR. The trend of taking part in dFFR in the mornings is reflected through a high SoC of 60-70% whereas the BM action in later blocks of the day is revealed as a sharp drop to 40% in the 33rd SP (i.e. 16:30 which is near the peak demand in evenings). The increase in SoC after the 40th SP (i.e. 20:00) complies with the observation that the bid prices are usually the lowest in Block 6 which results in an opportunity to recharge and start the next day with an SoC higher or equal to 50%. This ensures that the dFFR opportunity in the first blocks of the day is not missed due to the "less than 50%" criteria displayed in Fig. 7.

4.3 Economic Analysis

This subsection presents the results obtained to investigate the economic viability of purchasing a 1MW/1MWh BESS for optimised tendering of dFFR and BM services. The net present value assessment had several factors with high sensitivity as discussed in [40] and [41]. A vital consideration is the discount rate which seems to range between 3.5-10% in numerous online sources regarding energy storage investments in the UK and is suggested to be 6% for

BESS by Jones *et al.* [41]. As the effect of discounting is higher on the cash flow, 6 and 4% were adopted for the cash flow and OPEX respectively. The CAPEX was calculated using the costs provided by a BESS manufacturer.

For instance, if the operational life of a 1MW/1MWh BESS started on the 1st of January 2019, it should break even in May 2028 before its warranty ends at the end of 2028. The payback period is exactly 112 months (i.e. 9 years and 4 months). If the BESS was decommissioned after 10 years of operation, its net present value (NPV) at the end of 2029 would be £30,000. If a similar pattern of operation was continued till 2032, the NPV would be £133,000.

5 Levelised cost of storage

The costs of different energy storage technologies vary greatly depending on several factors that range from the method of storage to manufacturing costs. Similar to the levelised cost of energy, the levelised cost of storage (LCOS) is a measure that allows comparison between different energy storage units. In this paper, it was used as a method of validation by comparing the LCOS calculated for the 1MW/1MWh BESS with the range provided by Julch [40] and the American asset management company Lazard [42]. As shown in 12, LCOS is an expression of the capital, discounted O&M and recharging costs per unit of power exported (where the export power is also discounted). Following Julch [40], the following formula was used to evaluate the levelised cost of the proposed BESS. CAPEX is a sum of power and energy capital costs, OPEX refers to O&M–related costs, C_c is the cost of electricity bought, E_d is the amount of energy discharged in MWh, i is the discount rate and lastly y is the operation period in years–shown in (12).

$$LCOS = CAPEX + \frac{\sum_{y=1}^{10}\left(\frac{OPEX + C_c}{(1+i)^y}\right)}{\sum_{y=1}^{10}\left(\frac{E_d}{(1+i)^y}\right)} \quad (12)$$

Using the LCOS formula in (12), the cost of proposed BESS was calculated to be £210/MWh which is lower than storage systems that use Hydrogen, Methane, Lead Acid and Flow batteries [40]. The LCOS found for each lithium-ion BESS investigated are within the maximum and minimum predictions by Julch [40] and Lazard [42] – as presented in Fig. 11. This also validates the accuracy and reliability of the simulation results as it complies with the range published by Julch [40]. In comparison to the pumped hydro storage (PHS) which accounts for 99% of the installed energy storage capacity, the cost of BESS is 10 times higher in terms of energy capital cost [27]. However, the power capital cost of BESS is less than half of the PHS cost [27].

Month		Block 1	2	3	4	5	6
Jan	WD	dFFR	dFFR	dFFR	dFFR	BM	BM
	NWD	dFFR	dFFR	dFFR	dFFR	BM	BM
Feb	WD	dFFR	dFFR	dFFR	dFFR	BM	BM
	NWD	dFFR	dFFR	dFFR	dFFR	dFFR	BM
Mar	WD	dFFR	dFFR	dFFR	dFFR	BM	BM
	NWD	dFFR	dFFR	dFFR	dFFR	BM	BM
Apr	WD	dFFR	dFFR	dFFR	dFFR	dFFR	BM
	NWD	dFFR	dFFR	dFFR	dFFR	dFFR	BM
May	WD	dFFR	dFFR	dFFR	BM	BM	BM
	NWD	dFFR	dFFR	dFFR	dFFR	dFFR	BM
Jun	WD	dFFR	dFFR	dFFR	dFFR	BM	BM
	NWD	dFFR	dFFR	dFFR	dFFR	BM	BM
Jul	WD	dFFR	dFFR	dFFR	dFFR	BM	BM
	NWD	dFFR	dFFR	dFFR	dFFR	BM	BM
Aug	WD	dFFR	dFFR	dFFR	dFFR	dFFR	BM
	NWD	dFFR	dFFR	dFFR	dFFR	BM	BM
Sep	WD	dFFR	dFFR	dFFR	dFFR	BM	BM
	NWD	dFFR	dFFR	dFFR	dFFR	BM	BM
Oct	WD	dFFR	dFFR	dFFR	dFFR	BM	BM
	NWD	dFFR	dFFR	dFFR	dFFR	BM	BM
Nov	WD	dFFR	dFFR	dFFR	dFFR	BM	BM
	NWD	dFFR	dFFR	dFFR	dFFR	BM	BM
Dec	WD	dFFR	dFFR	dFFR	dFFR	BM	BM
	NWD	dFFR	dFFR	dFFR	dFFR	BM	BM

Fig. 9: Matrix of services shows the optimised service participation for each block of working (WD) and non-working (NWD) day profiles of each month

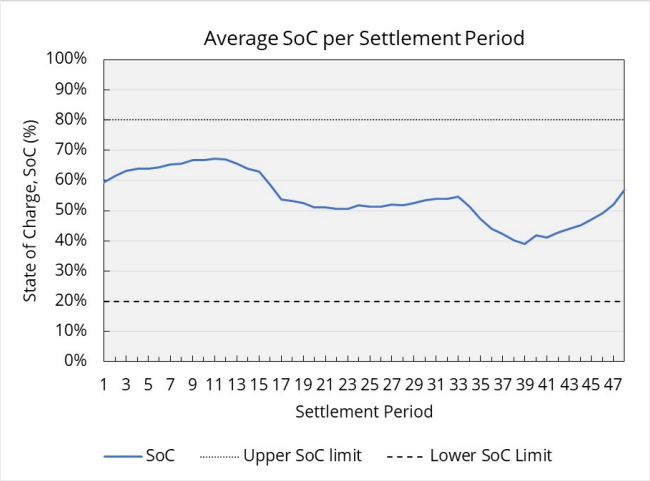

Fig. 10: Average SoC per SP when the BESS is participating in both dFFR and BM

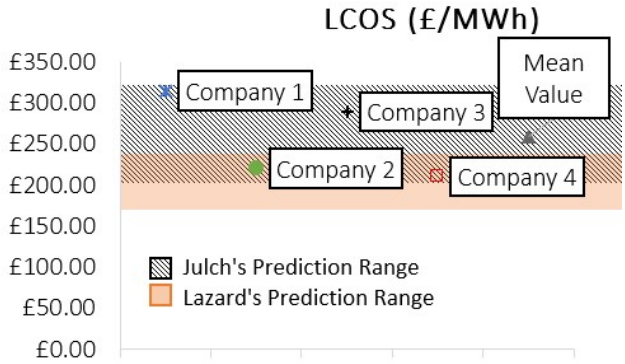

Fig. 11: Comparison of LCOS values calculated using the information provided by 4 different li-ion BESS companies with the ranges advised by Julch [40] and Lazard [42]

6 Conclusion

The proposed BESS system and service participation is able to take part in faster balancing action such as BM and dFFR in order to stabilise the system frequency and deliver electricity within the regulatory range within a smart grid infrastructure. In addition to being a relatively low-carbon solution in comparison to the conventional means of response (i.e. operating fossil-fuel generators at part-load [30]), the proposed scheme has an NPV of £30k by the end of its lifetime with a payback period of 9 years and 4 months. These numbers were attained through mathematical optimisation of the service participation which resulted in a net profit that is 70% and 20% higher than the sole participation in BM and dFFR respectively. Participation in these services was simulated using *BM Simulator* 1.0 and *dFFR Simulator* 1.0 which are described in Section 3. By combining the real historic data (i.e. system imbalance pricing and frequency data) with service regulations and constraints, both simulators output number of cycles completed and profit gained. In order to produce

the most optimal and profitable despatch schedule for participation in both services, Particle Swarm Optimisation algorithm was deployed in conjunction with various technical and operational constraints which include 60% depth of discharge, 5000 cycle lifetime and numerous service regulations.

As a result of the optimised despatch schedule, the overall capacity of the battery was degraded to 71% after 10 years, employing a dynamic degradation. The dynamic degradation model employed the curve fitting technique and used real usage data from the BESS industry. Using a constrained optimisation method enabled operation within 500 cycles per year which ensured a 10-year warranty. 84% of the total benefit originated from the BM service whilst dFFR contributed 16%. Only 30% of the total time was spent engaged in BM action, in comparison to 70% spent taking part in dFFR. In contrast, the majority of the cycles (i.e. 88%) were completed when participating in BM. The implication of the results is that despite the higher technical degradation of BM action, using the proposed despatch scheduler accompanied with historic data would result in 20% higher profit overall than just dFFR whilst occupying less than a third of the total active time.

Using the levelised cost of the storage method, the cost of the proposed BESS was calculated to be £210/MWh which is lower than storage systems that use Hydrogen, Methane, Lead Acid and Flow batteries. This value is also used to validate the accuracy and reliability of the simulation results as it complies with the range suggested by Julch [40]. Fast balancing actions such as dFFR and BM are expected to increase in value as the generation capacity of renewable energy technologies grow. Meanwhile, the cost of lithium-ion BESS is anticipated to decrease as investment and innovation persist in the field of storage. Both of these factors would result in a lower LCOS of lithium-ion BESS in the future, making it more economically attractive.

It is anticipated that the optimised pattern of operation, dynamic lifetime degradation and economic service analysis demonstrated in this paper would be the basis for more sophisticated studies and the motivation for further investment in lithium-ion BESS for making the grid smarter and more resilient. This methodology would allow more load and generation, including renewable energy technologies, to be connected to the existing grid without the associated cost of infrastructure development. This would particularly benefit countries with a developing grid infrastructure. Hence, it would be beneficial for future work to perform similar simulations using a developing country as a case study (i.e. use real frequency data, BM market data, regulations, etc. as inputs into the simulators). The service regulations could also be altered to compare various other options. Another future contribution could include modelling different types of the energy storage and their participation in the services whilst respecting their technical and operational constraints. Additionally, if the objectives of the optimisation are different such as SoC management and state of health, the same simulators can be used and the COF can be redefined to suit the chosen objectives.

Despite the fact that not all frequency and imbalance events can be linked back to the intermittency problem of renewable energy generation, in a system where stability is almost inversely related to the renewable energy generation, batteries and other types of energy storage are expected to become even more valued.

7 Acknowledgements

The authors would like to acknowledge the support of the Engineering and Physical Sciences Research Council (EPSRC) Doctoral Training Partnership [EP/R513209/1], the EPSRC National Centre for Energy Systems Integration (CESI) [EP/P001173/1] and Data-Driven Intelligent Energy Management for Environmentally Sustainable Energy Access (D-DIEM) Project supported by the British Council, UK-India Education and Research Initiative and the Indian Department of Science and Technology [16/17-19].

8 References

[1] National Grid: 'System needs and product strategy', 2017

[2] Kim, Y., Raghunathan, V., Raghunathan, A.: 'Design and management of hybrid electrical energy storage systems for regulation services', *Int. Green Comput. Conf.*, 2014, pp. 1–9

[3] Pan, X., Xu, H., Song, J., *et al.*: 'Capacity optimization of battery energy storage systems for frequency regulation', *2015 IEEE Int. Conf. Autom. Sci. Eng.*, 2015, pp. 1139–1144

[4] Doherty, R., Mullane, A., Nolan, G., *et al.*: 'An assessment of the impact of wind generation on system frequency control', *IEEE Trans. Power Syst.*, **25**, (1), 2010, pp. 452–460

[5] Toge, M., Kurita, Y., Orni, T., *et al.*: 'LFC with storage battery considering SOC for large-scale wind power penetration', *Asia-Pacific Power Energy Eng. Conf. APPEEC*, 2015

[6] Vergnol, A., Rious, V., Sprooten, J., *et al.*: 'Integration of renewable energy in the European power grid: market mechanism for congestion management', *Energy Mark. (EEM), 2010 7th Int. Conf. Eur.*, 2010, pp. 1–6

[7] Gortz, S.: 'Battery energy storage for intermittent renewable electricity production: A review and demonstration of energy storage applications permitting higher penetration of renewables', 2015

[8] Gils, H. C., Scholz, Y., Pregger, T., *et al.*: 'Integrated modelling of variable renewable energy-based power supply in Europe', *Energy*, **123**, 2017, pp. 173–188

[9] Sami, S. S., Cheng, M., Wu, J.: 'Modelling and control of multi-type grid-scale energy storage for power system frequency response', *2016 8th IEEE Int. Power Elect. and Motion Cont. Conf. (IPEMC-ECCE Asia)*, 2016, pp. 269–273

[10] ABB: 'Case note: Battery energy storage PCS solution for EKZ, one of Switzerland's largest energy companies', 2018, pp. 1–4. Available at https://library.e.abb.com/public/3787d20c96b13c6783257c5a007b5540/EKZ-CaseNote-PEBESS-PHFC03U-EN-web.pdf, accessed 16 May 2019

[11] Gundogdu, B. M., Nejad, S., Gladwin, D. T., *et al.*: 'A battery energy management strategy for UK enhanced frequency response and triad avoidance', *IEEE Trans. Ind. Electron.*, **65**, (12), 2018, pp. 9509–9517

[12] Duggal, I., Venkatesh, B.: 'Short-term scheduling of thermal generators and battery storage with depth of discharge-based cost model', *IEEE Trans. Power Syst.*, **30**, (4), 2015, pp. 2110–2118

[13] Rosewater, D., Ferreira, S.: 'Battery energy storage state-of-charge forecasting: models, optimization, and accuracy', *IEEE Trans. Smart Grid*, **10**, (3), 2018, pp. 2453–2462

[14] Liu, K., Chen, Q., Kang, C., *et al.*: 'Optimal operation strategy for distributed battery aggregator providing energy and ancillary services', *J. Mod. Power Syst. Clean Energy*, **6**, (4), 2018, pp. 722–732

[15] Kazemi, M., Zareipour, H., Amjady, N., *et al.*: 'Operation scheduling of battery storage systems in joint energy and ancillary services markets', *IEEE Trans. Sustain. Energy*, **8**, (4), Oct. 2017, pp. 1726–1735

[16] Sarker, M. R., Pandzic, H., Ortega-Vazquez, M. A.: 'Optimal operation and services scheduling for an electric vehicle battery swapping station', *IEEE Trans. Power Syst.*, **30**, (2), 2015, pp. 901–910

[17] Ansari, M., Al-Awami, A. T., Sortomme, E., *et al.*: 'Coordinated bidding of ancillary services for vehicle-to-grid using fuzzy optimization', *IEEE Trans. Smart Grid*, **6**, (1), 2015, pp. 261–270

[18] Motalleb, M., Thornton, M., Reihani, E., *et al.*: 'Providing frequency regulation reserve services using demand response scheduling', *Energy Conv. and Man.*, **124**, (15), 2016, pp. 439–452

[19] Greenwood, D., Wade, N., Taylor, P., *et al.*: 'A forecasting, optimization and scheduling system for energy storage systems in distribution networks', *2016 IEEE Power and Energy Soc. Gen. Meet. (PESGM)*, 2016, pp. 1–5

[20] Taylor, Z., Akhavan-Hejazi, H., Cortez, E., *et al.*: 'Customer-side SCADA-assisted large battery operation optimization for distribution feeder peak load shaving', *IEEE Trans. Smart Grid*, **10**, (1), 2017, pp. 992-1004

[21] Jinlei, S., Lei, P., Ruihang, L., *et al.*: 'Economic operation optimization for 2nd use batteries in battery energy storage systems', *IEEE Access*, **7**, 2019, pp. 41852–41859

[22] Rodriguez-Gallegos, C. D., Gandhi, O., Yang, D., *et al.*: 'A siting and sizing optimization approach for PV-battery-diesel hybrid systems', *IEEE Trans. Ind. App.*, **54**, (3), 2018, pp. 2637–2645

[23] Abdolrasol, M. G. M., Hannan, M. A., Mohamed, A., *et al.*: 'An optimal scheduling controller for virtual power plant and microgrid integration using the binary backtracking search algorithm', *IEEE Trans. Ind. App.*, **54**, (3), 2018, pp. 2834–2844

[24] Shang, C., Srinivasan, D., Reindl, T.: 'An improved particle swarm optimisation algorithm applied to battery sizing for stand-alone hybrid power systems', *Int. J. Elect. Power Energy Syst.*, **74**, 2016, pp. 104–117

[25] Greenwood, D. M., Lim, K. Y., Patsios, C., *et al.*: 'Frequency response services designed for energy storage', *Appl. Energy*, **203**, 2017, pp. 115–127

[26] Pop, V., Bergveld, H. J., Danilov, D., *et al.*: 'Battery management systems: accurate state-of-charge indication for battery-powered applications' (Springer Netherlands, Eindhoven, 2008)

[27] Sabihuddin, S., Kiprakis, A. E., Mueller, M.: 'A numerical and graphical review of energy storage technologies', *Energies*, **8**, (1), 2015, pp. 172–216

[28] Cho, J., Jeong, S., Kim, Y.: 'Commercial and research battery technologies for electrical energy storage applications', *Prog. Energy Combust. Sci.*, **48**, 2015, pp. 84–101

[29] Kempton, W., Tomic, J.: 'Vehicle-to-grid power implementation: from stabilizing the grid to supporting large-scale renewable energy', *J. Power Sources*, **144**, (1), 2015, pp. 280–294

[30] Kim, K., Choi, Y., Kim, H.: 'Data-driven battery degradation model leveraging average degradation function fitting', *Electron. Lett.*, **53**, (2), 2017, pp. 102–104

[31] Gao, Y., Jiang, J., Zhang, C., *et al.*: 'Lithium-ion battery aging mechanisms and life model under different charging stresses', *J. Power Sources*, **356**, 2017, pp. 103–114

[32] Ando, K., Matsuda, T., Imamura, D.: 'Degradation diagnosis of lithium-ion batteries with a LiNi0.5Co0.2Mn0.3O2 and LiMn2O4 blended cathode using dV/dQ curve analysis', *J. Power Sources*, **390**, 2018, pp. 278–285
[33] Narayanrao, R., Joglekar, M. M., Inguva, S.: 'A phenomenological degradation model for cyclic aging of lithium ion cell materials', *J. Electrochem. Soc.*, **160**, (1), 2012, pp. A125–A137
[34] Mckissock, B. I., Manzo, M. A., Miller, T. B., *et al.*: 'Progress of ongoing NASA lithium-ion cell verification testing for aerospace applications', 2008. Available at https://ntrs.nasa.gov/archive/nasa/casi.ntrs.nasa.gov/20080022410.pdf, accessed 16 May 2019
[35] National Grid: 'Fast reserve service description', 2013, pp. 1–20. Available at https://so-ups.ru/fileadmin/files/company/markets/dr/national_grid/dr_national_grid_1_13.jpg.pdf, accessed 16 May 2019
[36] Elexon: 'Imbalance pricing guidance', 2013, pp. 1–50. Available at https://www.elexon.co.uk/documents/training-guidance/bsc-guidance-notes/imbalance-pricing/, accessed 16 May 2019
[37] Chavez, H., Baldick, R., Sharma, S.: 'Governor rate-constrained OPF for primary frequency control adequacy', *IEEE Trans. Power Syst.*, **29**, (3), 2014, pp. 1473–1480
[38] National Grid: 'Enhanced frequency control capability (EFCC)', 2015. Available at https://www.nationalgrideso.com/document/96486/download, accessed 16 May 2019
[39] Jerald, J., Asokan, P., Prabaharan, G., *et al.*: 'Scheduling optimisation of flexible manufacturing systems using particle swarm optimisation algorithm', *Int. J. Adv. Manuf. Technol.*, **25**, 2005, pp. 964–971
[40] Julch, V.: 'Comparison of electricity storage options using levelized cost of storage (LCOS) method', *Appl. Energy*, **183**, 2016, pp. 1594–1606
[41] Jones, C., Peshev, V., Gilbert, P., *et al.*: 'Battery storage for post-incentive PV uptake? A financial and life cycle carbon assessment of a non-domestic building', *J. Cleaner Production*, **167**, 2017, pp. 447–458
[42] Lazard: 'Lazard's levelized cost of energy analysis 3.0', 2017. Available at https://www.lazard.com/media/450338/lazard-levelized-cost-of-storage-version-30.pdf, accessed 16 May 2019